Temporal changes in coda Q-1 and b value due to the static stress change associated with the 1995 Hyogo-ken Nanbu earthquake

著者	Hiramatsu Yoshihiro, Hayashi Nobuhiko, Furumoto Muneyoshi
journal or publication title	Journal of Geophysical Research B: Solid Earth
volume	105
number	3
page range	6141-6151
year	2000-03-10
URL	http://hdl.handle.net/2297/33411

JOURNAL OF GEOPHYSICAL RESEARCH, VOL. 105, NO. B3, PAGES 6141–6151, MARCH 10, 2000

Temporal changes in coda Q^{-1} and b value due to the static stress change associated with the 1995 Hyogo-ken Nanbu earthquake

Yoshihiro Hiramatsu, Nobuhiko Hayashi,[1] and Muneyoshi Furumoto
Department of Earth Sciences, Faculty of Science, Kanazawa University, Kakuma, Kanazawa, Japan

Hiroshi Katao
Research Center for Earthquake Prediction, Disaster Prevention Research Institute
Kyoto University, Gokasho, Uji, Japan

Abstract. The seismicity in the Tamba region, northeast of the Hyogo-ken Nanbu earthquake in Japan (January 17, 1995; M_{JMA} 7.2), increased significantly following this earthquake. This increase suggests that the static stress change due to a large earthquake causes a change in the crustal condition or dynamics. In order to reveal the changes quantitatively, we investigate the temporal variation in coda Q^{-1} and b value in the Tamba region. We analyze the waveform data of many shallow microearthquakes (M 1.5–3.0) in the region recorded in a period from 1987 to 1996. Coda Q^{-1} is estimated in 10 frequency bands in a range of 1.5–24 Hz based on the single isotropic scattering model. At frequencies between 1.5 and 4.0 Hz the temporal variation in coda Q^{-1} shows significant correlation with the occurrence of the Hyogo-ken Nanbu earthquake; coda Q^{-1} increases after the event. A variation in b value whose sign is opposite to that of coda Q^{-1} is recognized. The fracture dimensions of microearthquakes that contribute to the variation in b value are estimated to be 400 m. This scale length is consistent with the characteristic scale length of scatterer, 300–600 m, which contributes effectively to a temporal variation in coda Q^{-1}. The crustal activity in the Tamba region is possibly controlled by the heterogeneity with dominant scale of 10^2 m. The stress sensitivity of the coda Q^{-1} change is estimated to be 10 $(\mathrm{MPa})^{-1}$. This value is an order of magnitude larger than the stress sensitivity of seismic velocity reported before.

1. Introduction

Coda Q^{-1}, or Q_C^{-1}, is measured from the decay rate of the coda waves recorded at local distances which are composed of S to S backscattering waves generated by heterogeneities in the lithosphere [*Aki*, 1980]. The value of coda Q^{-1} correlates with the tectonic activity; high and low Q_C^{-1} values are obtained in active regions and stable regions, respectively [*Singh and Herrmann*, 1983]. The frequency dependence of coda Q^{-1} ($\propto f^{-n}$, where f is the frequency and n is a constant) also correlates with the tectonic activity well. The value of n is large for active regions and small for stable regions [*Singh and Herrmann*, 1983].

A temporal change in coda Q^{-1} was first found by *Chouet* [1979] in central California. Since then, many papers which report an increase or decrease in coda Q^{-1} before major earthquakes have been published (see a brief review by *Jin and Aki* [1989]). Also various high-resolution studies using doublets have observed no significant change in coda Q^{-1} associated with the Loma Prieta earthquake [*Beroza et al*., 1995] or during the earthquake cycle [*Aster et al*., 1996; *Antolik et al*., 1996]. Furthermore, it is observed that the temporal variation in coda Q^{-1} is associated with the variation in b value of the magnitude-frequency relation of earthquakes and other parameters reflecting the crustal condition [*Jin and Aki*, 1986; *Robinson*, 1987]. *Jin and Aki* [1989] found a large and systematic temporal variation in coda Q^{-1} and positive correlation with that in seismicity in southern California from 1933 to 1987, which led them to the construction of the creep model for the temporal variations. These observations suggest that the detection of the temporal variations in coda Q^{-1} and b value can be a powerful tool for earthquake prediction [*Aki*, 1985]. However, further work is required to understand the relation among coda Q^{-1}, b value, and the stress conditions.

The 1995 Hyogo-ken Nanbu earthquake in Japan (M_{JMA} 7.2) provides high-quality data with which to study the variations in coda Q^{-1} and b value produced by a stress change in the crust. In this study we carefully examine the response of coda Q^{-1} and b value due to the static stress change in the Tamba region, which is located to the northeast of the mainshock rupture zone.

2. Tectonic and Seismic Features in the Tamba Region

The Tamba region is located in central Honshu, Japan (Figure 1). This region has the densest distribution of Quaternary active faults in Japan and has very high seismicity (Figure 1). The seismicity in this region has been high for several decades, providing good data for an investigation of coda Q^{-1} and b

[1]Now at Fujitsu FIP Co., Nagoya, Japan.

Paper number 1999JB900432.
0148-0227/00/1999JB900432$09.00

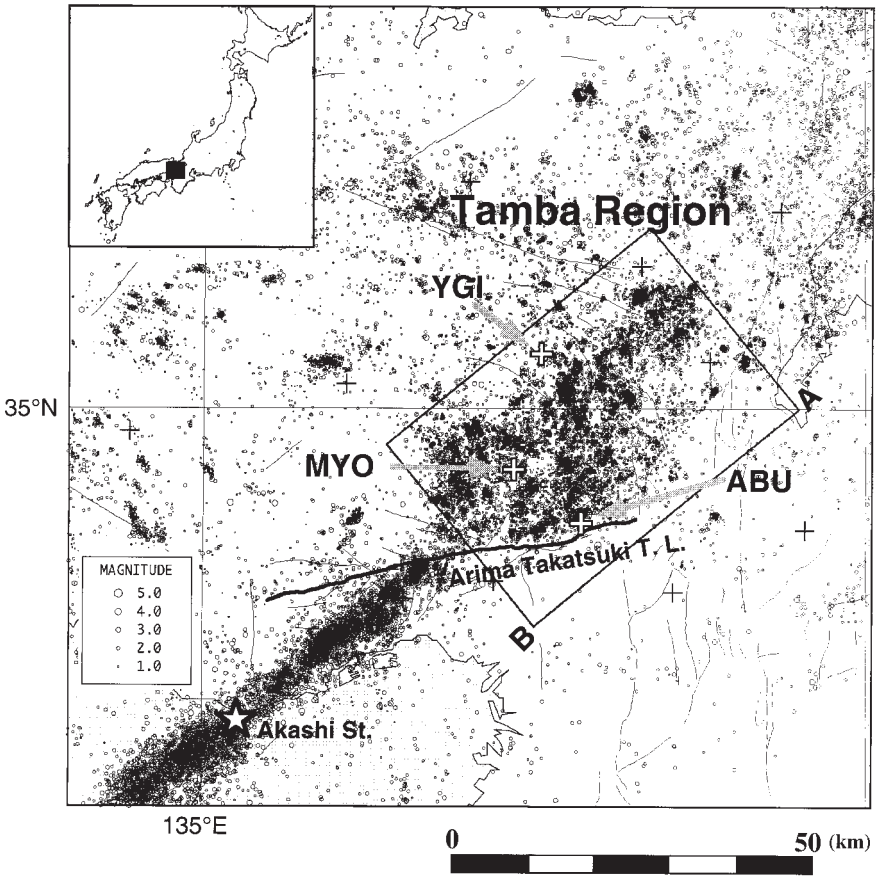

Figure 1. The distribution of epicenters in the depth range between 0 and 20 km (circles) and stations (crosses) from 1987 to 1996 in the Kinki district, central Honshu, Japan. The rectangle shows the Tamba region where we analyzed Q_C^{-1}. Star shows the epicenter of the Hyogo-ken Nanbu earthquake. Thin lines are Quaternary active faults. Line A-B denotes a section of the spatial-temporal plot of seismicity in Figure 2. Seismic stations: ABU, Abuyama; YGI, Yagi; MYO, Myokensan.

value. Microearthquakes have occurred not only along specific faults but also all over the Tamba region. The frequency of earthquakes increases with depth to above 12 km and then decreases at greater depth. The focal mechanisms vary from reverse and strike-slip to strike-slip [*Iio*, 1996]. Both types of focal mechanisms have a dominant P axis in nearly E-W orientation. *Iio* [1996] thus concluded that the brittle-semibrittle transition occurs at 12 km, corresponding to 300–350°C [*Ito*, 1990], in this region.

The Hyogo-ken Nanbu earthquake (M_{JMA} 7.2), a typical strike-slip event whose P axis trends nearly E-W, occurred on January 17, 1995, to the southwest of the Tamba region. The epicenter was located in the Akashi Strait, and the source depth was 17 km. The fault length was ~50 km, and the rupture propagation was bilateral [e.g., *Horikawa et al*., 1996]. Since the Hyogo-ken Nanbu earthquake, the seismicity in the Tamba region has increased (Figure 2). *Hashimoto* [1996, 1997] calculated the change in the Coulomb failure function ΔCFF due to the Hyogo-ken Nanbu earthquake using a fault model with six fault segments derived mainly from Global Positioning System (GPS) observations. He reported that the rapid increase of microearthquake activity in the Tamba region was induced by an increase in ΔCFF (~0.04 MPa for strike-slip faults trending N45°E and their conjugates). *Katao et al*. [1997] studied the focal mechanisms of microearthquakes in and around the rupture zone of the Hyogo-ken Nanbu earthquake in detail. They found no change in the direction of the regional stress field of the Tamba region after the Hyogo-ken Nanbu earthquake.

3. Data and Method

We use the waveform data recorded by Abuyama seismic station network, operated by Disaster Prevention Research Institute, Kyoto University. The locations of the stations in the region are shown in Figure 1 with the epicentral distribution of local microearthquakes. The stations of this network are equipped with three-component velocity seismometers with a natural frequency of 1.0 Hz. The waveform data are digitized at a sampling rate of 200 Hz and stored automatically by an event trigger recording system at Abuyama Observatory. The magnitude of each event is determined using the maximum amplitude of the vertical component recorded by the network [*Watanabe*, 1971].

To investigate the temporal variation in Q_C^{-1}, we use local earthquakes recorded January 1, 1987, to December 31, 1996, within the rectangle area (~50 km × 35 km) called the Tamba region, indicated in Figure 1. We analyze waveform data from the vertical component of three stations, Abuyama (ABU), Yagi (YGI), and Myokensan (MYO), which are operated con-

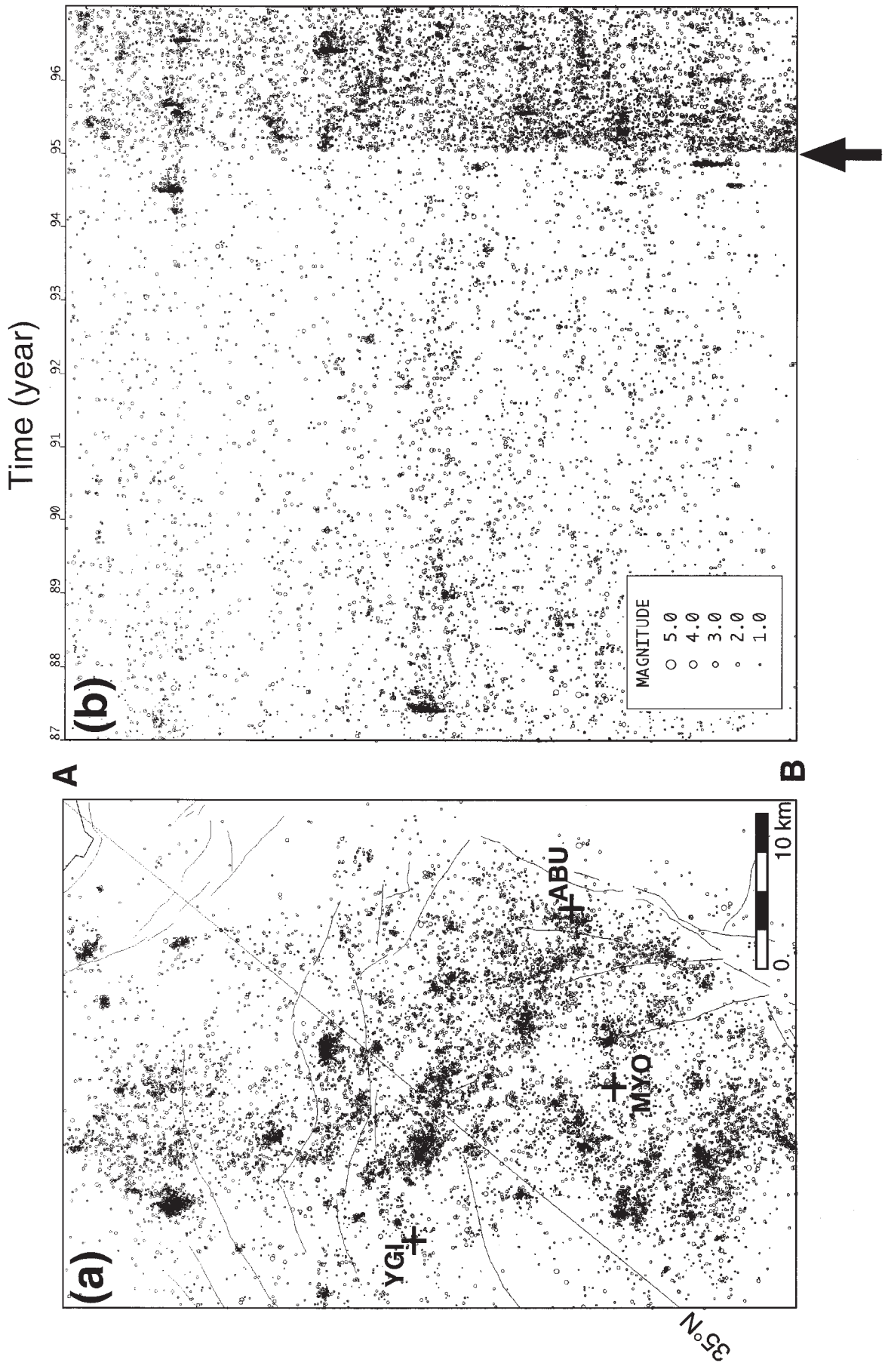

Figure 2. (a) The distribution of epicenters and (b) the spatial-temporal variation in seismicity in the analyzed area (section A-B on rectangle in Figure 1). Arrow shows the occurrence of the Hyogo-ken Nanbu earthquake. The change in seismicity associated with the Hyogo-ken Nanbu earthquake is clearly shown as the increase of earthquakes over the region.

tinuously through the whole analysis period and whose data quality is high enough to analyze Q_C^{-1}.

To estimate Q_C^{-1}, we required high-quality and unsaturated waveforms. For example, the surface waves from a very shallow earthquake contaminate the coda waves. In this study, only unsaturated waveforms of earthquakes satisfying the following conditions are used for the estimation of Q_C^{-1}: (1) The hypocentral distance is shorter than 40 km, (2) the magnitudes are <3.0, and (3) the depth is in the range of 5–15 km. Since most of the focal mechanisms of earthquakes in the study area are strike-slip and reverse with P axes of E-W orientation, so are the mechanisms of the selected earthquakes.

Coda Q^{-1} at a frequency f is estimated by the temporal decay of a band-pass-filtered coda signal whose central frequency is f. According to the single isotropic scattering model the coda amplitude approximated by the root mean square of the amplitude at a frequency f is given by the following formula [*Sato*, 1977]:

$$A_C(f|t) = -\ln t - \pi Q_C(f)^{-1} f t + \text{const}, \tag{1}$$

where $A_C(f|t)$ is the root-mean-square (RMS) amplitude of band-pass-filtered coda waves at a center frequency of f and lapse time of t. We use the band-pass-filtered data with center frequencies of 1.5, 2.0, 3.0, 4.0, 5.0, 6.0, 7.0, 8.0, 12.0, and 24.0 Hz and then calculate the RMS amplitude in a moving window with a duration of $4/f$ for each center frequency. We analyze the coda in a lapse time window from twice of the S wave travel time, $2T_S$, to 25 s after the origin time, because coda waves are little affected by the source mechanism after $2T_S$ but are affected by multiple scattering for a long lapse time [*Sato*, 1977; *Rautin and Khalturin*, 1978]. If the tail of the coda is shorter than 25 s, we regarded the time when the coda amplitude reaches twice of the noise level for each frequency band as the end of the time window. We eliminate data with high background noise levels or a time window shorter than twice of the periods. Simple least squares method is not appropriate to fit (1) to $A_C(f|t)$ for the estimation of Q_C^{-1}, because reflected phases occasionally disturb the monotonous coda decay, giving an unstable estimation of Q_C^{-1}. We apply the robust estimation by the criteria of the least absolute deviation to estimate Q_C^{-1} using (1). Q_C^{-1} is averaged over the three stations for each earthquake, and this average value is used in the following discussion on the temporal change in Q_C^{-1}.

The epicenters used for the estimation of the average Q_C^{-1} for each frequency band are shown in Figure 3, separately. For each frequency band the epicenters before and after the Hyogo-ken Nanbu earthquakes are plotted separately to examine the existence of a systematic difference of the epicentral distributions. There is no systematic difference between the two distributions in the individual frequency bands.

The lapse times of the ends of the time windows from the earthquake origin times are not constant in this study. The value of Q_C^{-1} in general depends on the lapse time [e.g., *Akamatsu*, 1980]. We can recognize a linear trend that the value of Q_C^{-1} is relatively higher for a short lapse time and lower for a long lapse time, especially for lower frequency bands. We remove the lapse time dependence of Q_C^{-1} by assuming a linear relation [*Hiramatsu et al.*, 1992],

$$\log Q_C^{-1} = c + dt, \tag{2}$$

where t is the lapse time. We use an average lapse time over the three stations for an earthquake as the lapse time as well as Q_C^{-1}. The coefficients c and d are determined by the least squares method (Table 1). We correct the value of Q_C^{-1} using equation (2), taking 20 s as the reference lapse time.

The temporal variation in b value is investigated in the same time period (1987–1996), the same area where Q_C^{-1} were estimated, and the same depth range. The number of earthquakes that occurred in the rectangle area in Figure 1 is counted at every 2 years for a magnitude interval of 0.1. The b value is determined by the maximum likelihood method [*Aki*, 1965]

$$b = \frac{\log e}{\bar{M} - M_{\min}}, \tag{3}$$

where $N(M)$ represents the total number of earthquakes with magnitudes greater than or equal to M and $\bar{M}$ is the average magnitude of a group of earthquakes with $M \geq M_{\min}$. A minimum magnitude $M_{\min}$ is determined to be 1.4 because the relation between $\log N(M)$ and M is linear above this magnitude through the whole period.

High seismic activity during swarms or aftershock sequences and their spatial variation may affect the estimation of b value. In order to estimate the b value of the background seismicity we remove remarkable clusters in 1987 and 1994 (Figure 2b) in the calculation of b value.

4. Temporal Variations in Coda Q^{-1} and b Value

Dividing the data into two periods, 8 years before and 2 years after the Hyogo-ken Nanbu earthquake, we investigate the change in the average values of coda Q^{-1} (Figure 4). The values of coda Q^{-1} for most frequency bands increased after the event, although their variations are within 1 standard deviation of the data. The increase of Q_C^{-1} is clearly shown for lower frequency bands. The Student's t test is used to examine for the temporal variation in the averages of Q_C^{-1} (Table 2). The differences in the averages of Q_C^{-1} between the two periods are significant for 1.5, 2.0, 3.0, 4.0, and 12.0 Hz with confidence level of 99%. Excepting the 12.0 Hz bands, all the Q_C^{-1} values of these frequency bands increased after the Hyogo-ken Nanbu earthquake.

Systematic changes in focal mechanisms, epicenters, and/or focal depths can cause a false temporal change in coda Q^{-1} [*Sato*, 1988]. Most focal mechanisms of earthquakes used in this study are strike-slip and reverse faults with P axes of E-W orientation, and no changes in focal mechanisms were reported [*Katao et al.*, 1997].

As shown in Figure 3, the epicentral distribution shows no large systematic variation between the periods before and after the Hyogo-ken Nanbu earthquake. Local changes in seismicity do occur, however, for example, a cluster around YGI. This high seismic activity occurred in the middle of 1987 as shown in Figure 2. In order to examine the effect of local changes in seismicity on the temporal change in coda Q^{-1} we divide the observation duration further into five periods of every 2 years (I–V). The change between the average Q_C^{-1} of period IV and period V represents the effect of the Hyogo-ken Nanbu earthquake. The variation of the averages and the variances of Q_C^{-1} for the five periods is listed in Table 3 for all the frequency bands. We can recognize that the average Q_C^{-1} increases between IV and V for lower frequencies again. We also find that the change in the average Q_C^{-1} prior to the mainshock (I–IV)

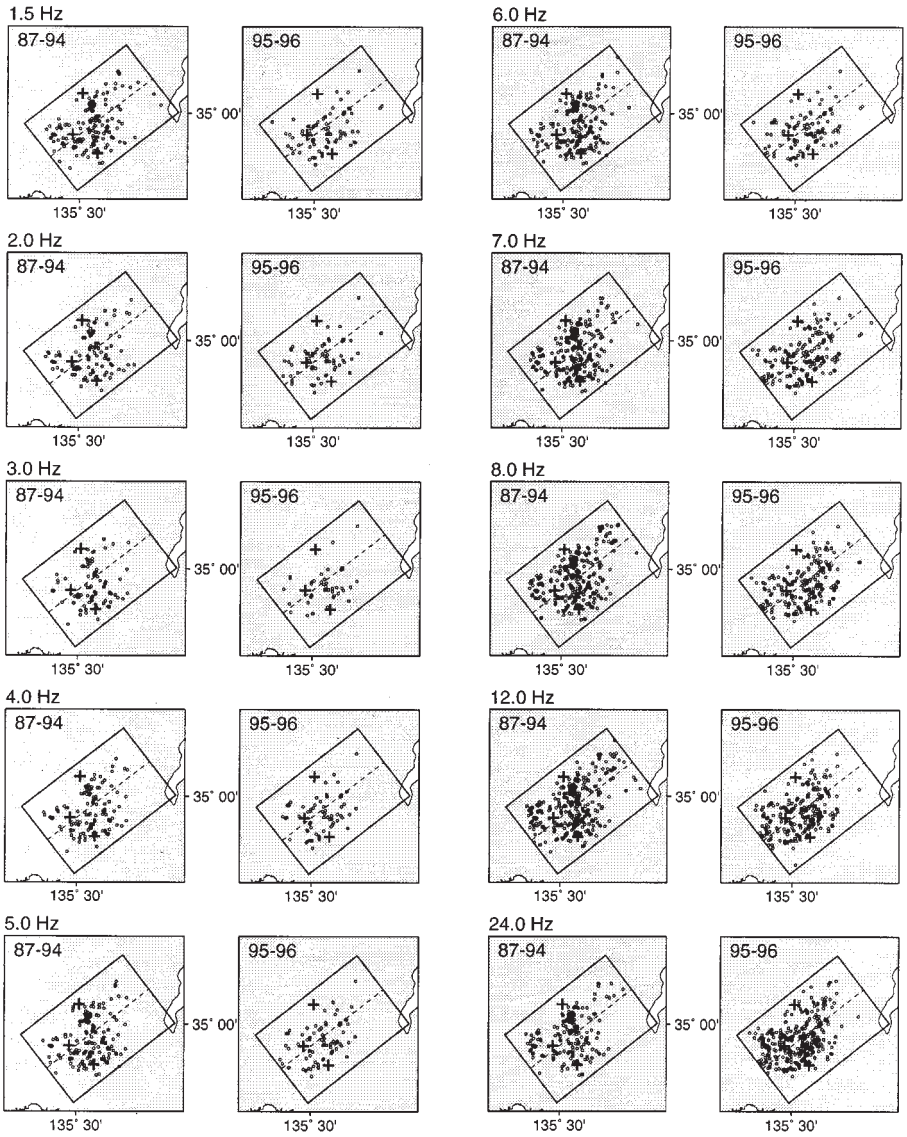

Figure 3. The epicentral distribution for earthquakes which are used for Q_C^{-1} analysis. For each frequency band the epicentral distribution is bounded by two periods, before the Hyogo-ken Nanbu earthquake and after it. No large systematic change in seismicity between the two periods is found for all frequency bands, indicating that the distribution of epicenters affects little the temporal variation in Q_C^{-1}. Dashed lines are the boundaries dividing the subregions, northern area and southern area, to examine the contribution of the variation in epicenters to those in coda Q_C^{-1} and b value.

Table 1. The Coefficients c and d of Equation (2) for Each Frequency Band

Frequency, Hz	c	d
1.5	−1.60	-1.43×10^{-3}
2.0	−1.72	-1.06×10^{-3}
3.0	−1.71	-1.94×10^{-3}
4.0	−2.01	-1.19×10^{-3}
5.0	−2.33	-1.88×10^{-3}
6.0	−2.46	4.71×10^{-4}
7.0	−2.50	-6.14×10^{-4}
8.0	−2.47	-3.73×10^{-3}
12.0	−2.58	-3.90×10^{-3}
24.0	−2.87	5.80×10^{-5}

appears to be random from frequency to frequency. In order to confirm the significance of the changes we apply the Student's t test again, comparing the average of Q_C^{-1} in each period with that of the following period. The results of t test for individual periods of all frequency bands are summarized in Table 3. The statistical test indicates that almost all changes of the average Q_C^{-1} between two successive periods are insignificant. Only the change in the average from period IV to V of 3.0 Hz and 4.0 Hz frequency bands (Figure 5) is significant with confidence level of 99%.

We examine the effect of local changes in seismicity on the temporal change in coda Q^{-1} by dividing the region into two subregions, northern and southern areas (see Figure 3). Figure

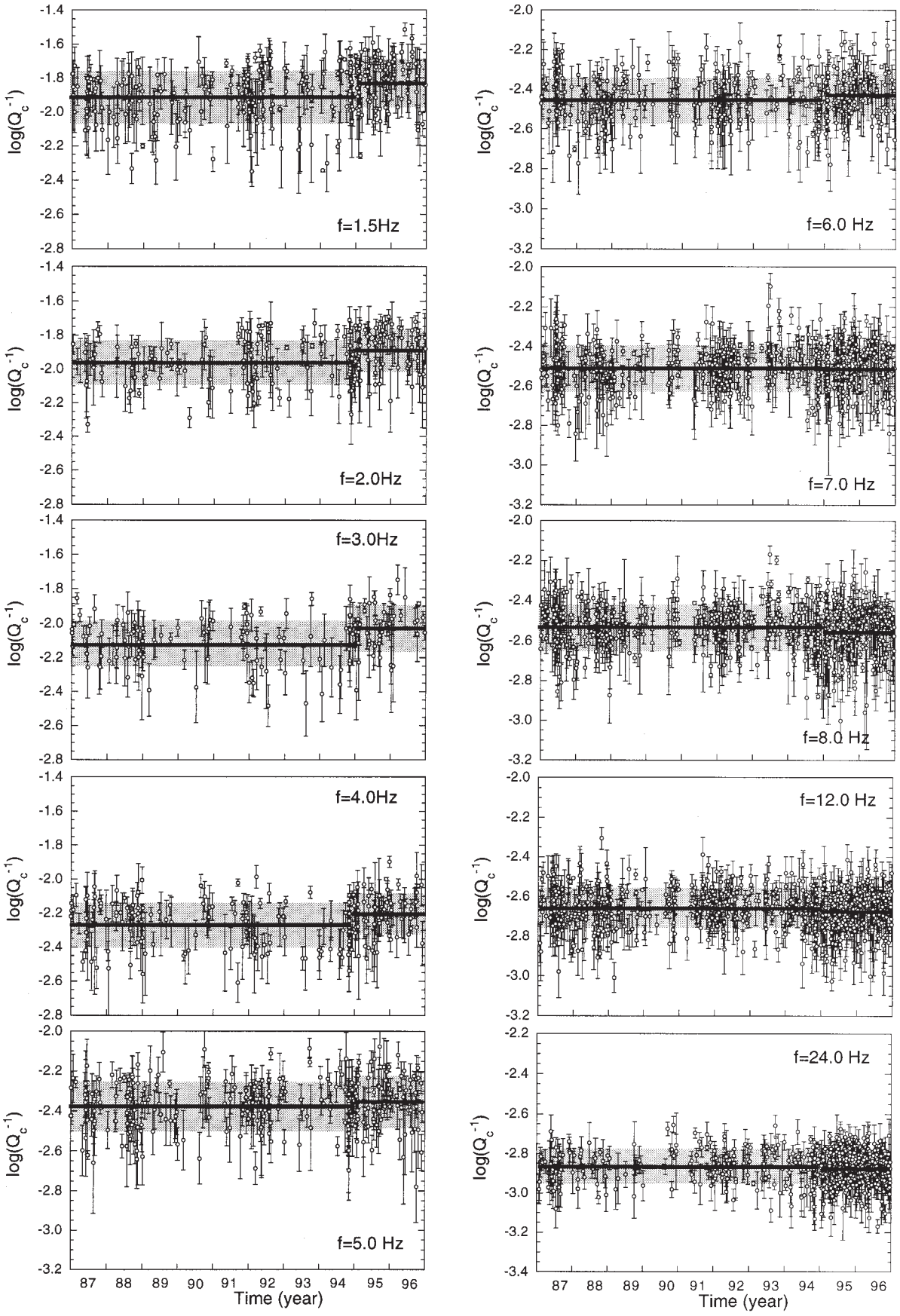

Figure 4. The temporal variation in Q_C^{-1} bounded by the occurrence of the Hyogo-ken Nanbu earthquake. Solid lines show the average, bars are the individual errors, and hatched zones are the standard deviation of data of each time window. At lower frequency bands the average of Q_C^{-1} increases after the earthquake.

Table 2. Summary of the Mean Values and the Standard Deviations of log (Q_C^{-1}) and the Results of the Statistical t Test

Frequency, Hz	Before			After			t Test, %
	$\log_{10}(Q_C^{-1})$	σ^2	Num	$\log_{10}(Q_C^{-1})$	σ^2	Num	
1.5	−1.91	0.023	197	−1.83	0.02	85	0.0
2.0	−1.96	0.017	126	−1.89	0.014	67	0.0
3.0	−2.12	0.018	107	−2.03	0.017	44	0.0
4.0	−2.27	0.017	148	−2.21	0.015	68	0.1
5.0	−2.38	0.015	196	−2.35	0.016	83	17.1
6.0	−2.46	0.014	250	−2.43	0.014	118	4.8
7.0	−2.51	0.013	322	−2.51	0.013	194	89.2
8.0	−2.53	0.012	387	−2.56	0.016	236	1.8
12.0	−2.65	0.01	455	−2.68	0.011	284	0.3
24.0	−2.87	0.007	224	−2.87	0.006	413	49.9

Num is the number of data. The data are bounded by the occurrence of the Hyogo-ken earthquake (Figure 4). The values of t test less than 0.5 show statistically the significance of the change with confidence level of 99.5%.

6 shows the temporal variations in Q_C^{-1} in each area in the 3.0 Hz and the 4.0 Hz frequency bands. The average value of Q_C^{-1} increases after the mainshock in both the areas, which is the same as that shown in Figure 4. For all frequencies we see similar temporal variations in Q_C^{-1} in each area as we observed in the whole region.

We were not able to identify any repeating events or doublets such as those used in the precise studies [*Beroza et al*., 1995; *Aster et al*., 1996; *Antolik et al*., 1996]. To investigate the effect of spatial changes, we therefore examine the variation in Q_C^{-1} of a series of earthquakes, which occurred steadily throughout the period, in a small volume (1 km × 1 km × 1 km) in this region. The average Q_C^{-1} increases after the mainshock at lower frequencies below 5.0 Hz although the number of data is small, less than 10. This variation is consistent with the variation in Q_C^{-1} shown in Figure 4. Thus the observed temporal change in Q_C^{-1} does not appear to result from a change in the distribution of epicenters.

The effect of the hypocentral depth on the temporal variation of coda Q^{-1} is also rejected as follows. Correlation between the focal depth and Q_C^{-1} in the individual frequency is examined by plotting observed Q_C^{-1} as a function of the focal depth. No significant or systematic correlation between the focal depth and Q_C^{-1} is observed; for example, a slight negative correlation is observed in the 3.0 Hz band, but a slight positive one is seen in the 4.0 Hz band. Therefore, even if a systematic temporal change of the focal depth occurred, it is unlikely to have caused the observed temporal change in coda Q_C^{-1}. Moreover, the average depth of the events used in this study is almost constant, 9–10 km, and there is no systematic change in the focal depth distribution with time from periods I through V.

We also investigate whether the frequency dependence of coda Q^{-1} varies with time. The frequency dependence of Q_C^{-1} is expressed by the power of frequency as

$$Q_c^{-1} = Q_0^{-1} f^{-n}, \tag{4}$$

where Q_0^{-1} is the Q_C^{-1} at 1 Hz and n is a constant. In order to determine the values of n for the individual periods I–V, relation (4) is fitted to the Q_C^{-1} values in the 10 frequency bands by the least squares method. Figure 7 shows the temporal variation in n. The value of n is lower before the Hyogo-ken Nanbu earthquake and higher afterward, but this increase in n is not statistically significant.

The b value in the Tamba region is shown in Figure 8. The overlap of 95% confidence levels shows that the variation in b value is not statistically significant from 1987 to 1994 (I–IV). However, the decrease in b value between IV and V is significant. We observe Q_C^{-1} to increase following the Hyogo-ken Nanbu earthquake, and so Q_C^{-1} appears to correlate negatively with b value in the Tamba region.

We also consider whether the b value varies with depth [*Mori and Abercrombie*, 1997]. We calculate b value every 2 km in depth and find a slight increase from a minimum of 0.92 ± 0.10 at the depth of 5–7 km to the maximum of 1.04 ± 0.05 at the depth of 11–13 km. This variation is too small to explain the observed temporal change in b value. Also, the depth distribution does not change with time during the analyzed period (I–V). We, furthermore, examine the effect of the spatial change in hypocenter on the temporal variation in b value by dividing the region into two subregions; we do the same for the case of Q_C^{-1}. In both areas the temporal variation in b value is similar to that in Figure 8.

5. Discussion

To summarize the observations described in section 4, coda Q^{-1} in the Tamba region shows a temporal variation before and after the Hyogo-ken Nanbu earthquake which negatively correlates with b value. In order to explain such a correlation between Q_C^{-1} and b value, *Jin and Aki* [1989] proposed the creep model. In their model, the stress increase tends to magnify the crack density and hence coda Q^{-1} in a seismic region. The fractures with a certain characteristic length a enhance occurrence of earthquakes of comparable size or characteristic magnitude M_c. Moreover, since the scattering of a seismic wave is most effective when a wavelength λ is comparable to twice the characteristic length of the scatterer by $\lambda \approx 2a$ [*Yomogida and Benites*, 1995], the increase of Q_C^{-1} should be largest in this characteristic wavelength band. If M_c is in the upper part of the magnitude range in the earthquake catalogue used to estimate b value, the enhancement of the seismicity results in a decrease of b value, and so a negative correlation between Q_C^{-1} in the characteristic wavelength band and b value is expected. This creep model is thus able to explain the negative correlation between Q_C^{-1} and b value observed in the Tamba region.

Figure 8 shows the temporal variation in the number of earthquakes for four magnitude ranges from 1.6 to 3.5 with an increment of 0.5, together with the variation in b value. The variations of the numbers of earthquakes in magnitude ranges

Table 3. Summary of the Mean Values and the Standard Deviations of log (Q_C^{-1}) and the Results of the Statistical t Test for Five Periods (I–V) of 2 Years

Frequency, Hz	Period	$\log_{10}(Q_C^{-1})$	σ^2	Num	t Test, %
1.5	I	−1.93	0.02	57	
1.5	II	−1.97	0.02	32	22.6
1.5	III	−1.89	0.02	56	2.1
1.5	IV	−1.89	0.03	50	95.6
1.5	V	−1.83	0.02	87	2.4
2.0	I	−1.98	0.01	31	
2.0	II	−1.99	0.01	22	76.0
2.0	III	−1.99	0.01	22	16.6
2.0	IV	−1.95	0.02	35	77.2
2.0	V	−1.89	0.01	70	2.3
3.0	I	−2.11	0.01	40	
3.0	II	−2.12	0.01	20	82.7
3.0	III	−2.13	0.02	23	65.3
3.0	IV	−2.14	0.03	21	87.8
3.0	V	−2.03	0.02	47	0.5
4.0	I	−2.24	0.02	53	
4.0	II	−2.27	0.02	24	32.3
4.0	III	−2.28	0.02	33	68.5
4.0	IV	−2.30	0.02	36	49.7
4.0	V	−2.20	0.02	70	0.0
5.0	I	−2.39	0.02	65	
5.0	II	−2.36	0.02	32	31.5
5.0	III	−2.37	0.01	52	91.8
5.0	IV	−2.37	0.02	46	68.0
5.0	V	−2.35	0.02	84	35.3
6.0	I	−2.47	0.01	86	
6.0	II	−2.43	0.01	38	10.8
6.0	III	−2.46	0.01	68	15.6
6.0	IV	−2.46	0.02	57	91.2
6.0	V	−2.43	0.01	119	15.8
7.0	I	−2.52	0.02	106	
7.0	II	−2.52	0.00	43	98.7
7.0	III	−2.52	0.00	92	78.3
7.0	IV	−2.49	0.02	81	10.2
7.0	V	−2.51	0.01	194	11.8
8.0	I	−2.53	0.01	134	
8.0	II	−2.53	0.00	49	81.0
8.0	III	−2.53	0.00	93	87.2
8.0	IV	−2.53	0.02	110	96.7
8.0	V	−2.56	0.02	237	9.1
12.0	I	−2.65	0.01	159	
12.0	II	−2.66	0.01	61	60.6
12.0	III	−2.64	0.00	114	30.7
12.0	IV	−2.66	0.00	120	13.8
12.0	V	−2.68	0.01	285	18.3
24.0	I	−2.88	0.00	65	
24.0	II	−2.85	0.00	24	10.0
24.0	III	−2.85	0.00	54	75.1
24.0	IV	−2.88	0.00	80	9.8
24.0	V	−2.87	0.00	414	58.1

See Figure 5. All symbols are the same as those of Table 2.

of M 2.6–3.0 and M 3.1–3.5 are larger than those in the other magnitude ranges. The variation in b value therefore reflects the variation in the activity of earthquakes with about M 3.0. This is in the upper part of the total magnitude range (1.6–3.5) and so may cause the negative correlation between Q_C^{-1} and b value.

We can compare the characteristic scale of the inhomogeneity inferred from the variation in Q_C^{-1} with the characteristic dimension of an M 3.0 earthquake. According to *Yomogida and Benites* [1995] the effective scale length a of inhomogeneities generating coda waves is nearly half of the wavelength. Assuming that S wave velocity in the crust is 2.5–3.5 km/s, the characteristic scale of the inhomogeneity is estimated to be 0.3–0.6 km for 3.0 and 4.0 Hz frequency bands.

Iio [1986] used the aftershock distributions of small to moderate earthquakes for $M > 3.0$ in Japan to determine a linear relation between the magnitude M and the fault length L (km) as follows:

$$\log L = 0.43M - 1.7. \quad (5)$$

Substituting $M = 3$, we obtain a fault length, which contributes to the variation in b value, of 0.4 km. This value is consistent with 0.3–0.6 km estimated from the wavelength of coda waves that show significant variation in Q_C^{-1}. These observations and the creep model [*Jin and Aki*, 1989] thus suggest that the inhomogeneity with characteristic scale of the order of 10^2 m is enhanced by the static stress change due to the Hyogo-ken Nanbu earthquake.

To estimate the degree of the stress change that causes the variations of Q_C^{-1} and b value, we calculate the static stress change associated with the Hyogo-ken Nanbu earthquake in the Tamba region in detail. All parameters are the same as those of *Hashimoto* [1997]. Figure 9 shows the change in the shear stress of N45°E, which is the strike of a nodal plane of most earthquakes in the Tamba region [*Katao et al.*, 1997], at the depth of 10 km. This indicates that the stress change is greater than 0.04 MPa only in the most southwest portion of Tamba region, while the stress change is small and at most 0.02 MPa in the rest of the area. Therefore the static stress change

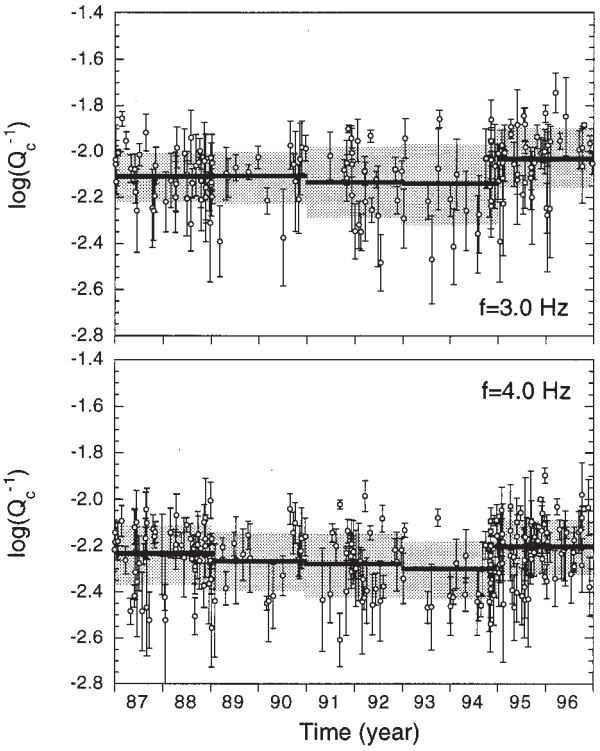

Figure 5. The temporal variation in Q_C^{-1} for five periods (I–V) of 2 years at the frequency bands of 3.0 and 4.0 Hz. Significant increase in Q_C^{-1} from IV to V corresponds to the occurrence of the Hyogo-ken Nanbu earthquake. All the symbols are the same as those in Figure 4.

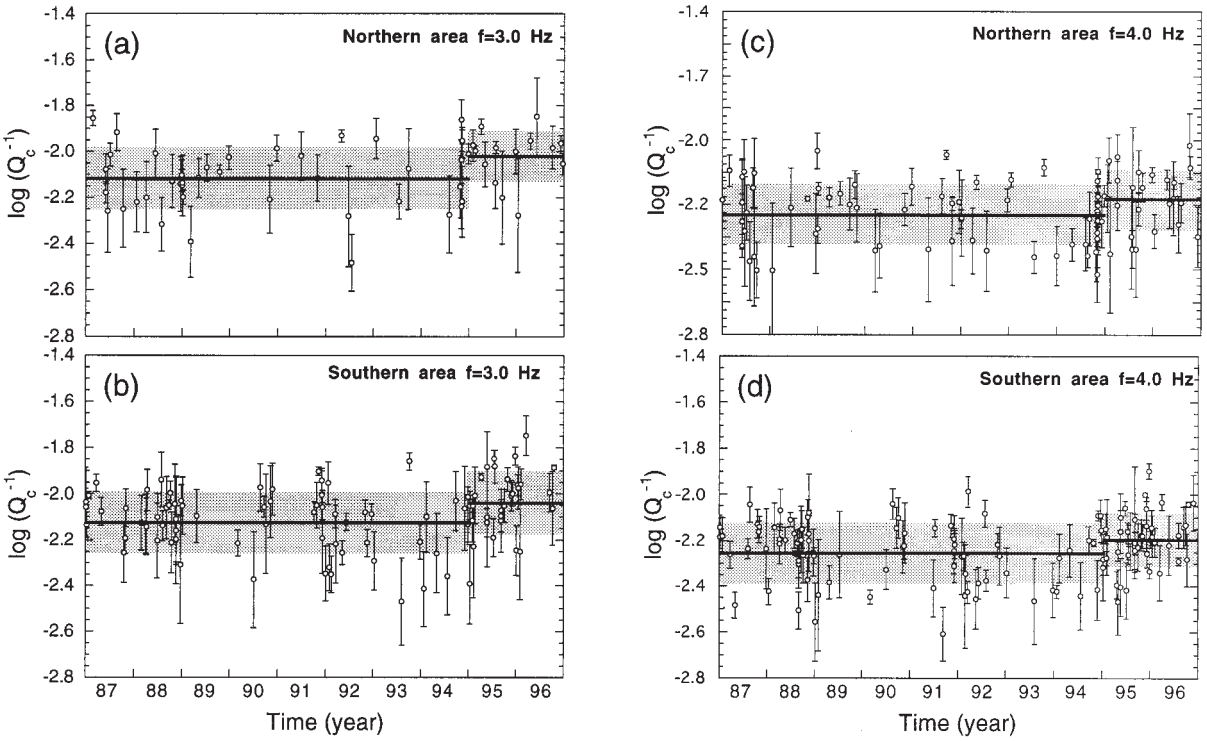

Figure 6. The temporal variation in Q_C^{-1} in (a and b) the northern and southern areas, respectively, in 3.0 Hz frequency band and (c and d) those in 4.0 Hz frequency band. All the symbols are the same as those in Figure 4.

of 0.02 MPa due to Hyogo-ken Nanbu earthquake is considered to be the cause of the changes in seismicity and Q_C^{-1}.

We define the sensitivity of coda Q^{-1} on the stress change (fractional change in coda Q^{-1}) as

$$-\frac{1}{Q_C^{-1}}\frac{dQ_C^{-1}}{d\tau}=\frac{1}{Q_C}\frac{dQ_C}{d\tau}, \tag{6}$$

where $d\tau$ is the stress change. The sensitivity around 3 and 4 Hz is calculated to be ~10 $(\text{MPa})^{-1}$. This value is much larger than the stress sensitivity of the seismic velocity in the crust reported before. *DeFazio et al.* [1973] estimated a stress-velocity coefficient of 1 $(\text{MPa})^{-1}$ in Franklin marble in situ by relating velocity variation to the Earth tide strain. *Reasenberg and Aki* [1974] repeated an air gun shot in a water-filled hole every 6 or 10 s to measure in situ seismic velocity over a distance of 200 m in a granite quarry. They estimated a stress-velocity coefficient of 2 $(\text{MPa})^{-1}$ by the correlation between velocity variation and the Earth tide. Therefore the stress sensitivity of coda Q^{-1} change estimated in this study is one order

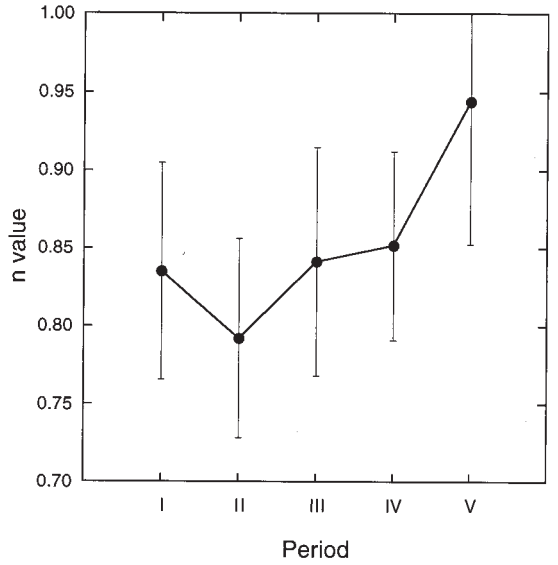

Figure 7. The temporal variation in the power of frequency n for Q_C^{-1}, showing almost constant value from I to IV and an increase in V, after the Hyogo-ken Nanbu earthquake. Bars show the confidence limits of 95%.

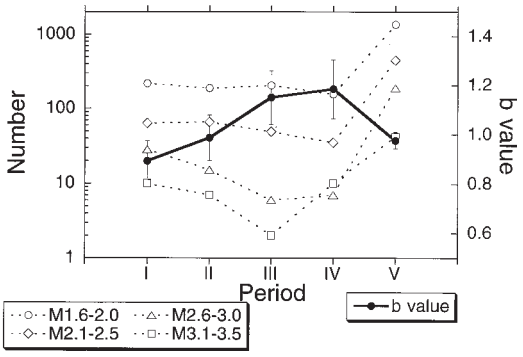

Figure 8. The temporal variation in b value (solid circles) and the number of earthquakes of four magnitude ranges: 1.6–2.0 (open circles), 2.1–2.5 (diamonds), 2.6–3.0 (triangles), and 3.1–3.5 (squares). Bars show the confidence limits of 95% of b value.

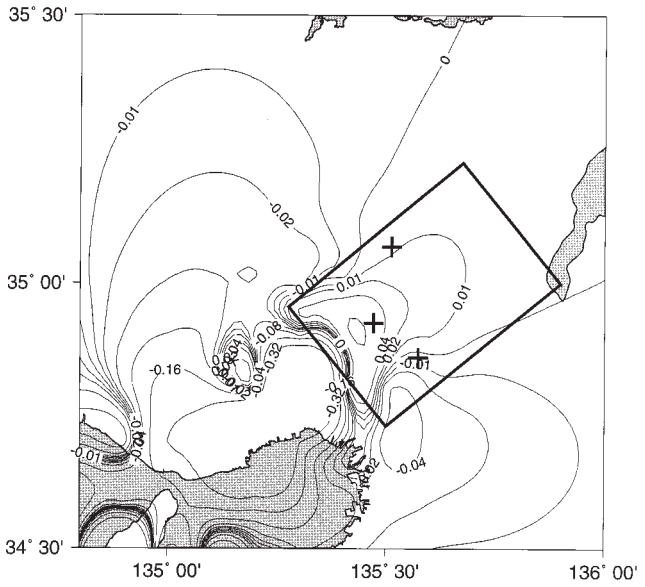

Figure 9. The change in the shear stress of the N45°E component at the depth of 10 km due to the Hyogo-ken Nanbu earthquake. Rectangle shows the analyzed area, and crosses show the stations for Q_C^{-1}. The fault model, geometry, and slip distribution of the mainshock of *Hashimoto et al*. [1996] are used. Poisson's ratio and rigidity are 0.25 and 40 GPa, respectively.

higher than that of seismic velocity. In other words, coda Q^{-1} may be a sensitive indicator of a stress change in the crust.

6. Conclusions

The response of Q_C^{-1} to the static stress change is confirmed by the analysis of coda waves from many microearthquakes before and after the 1995 Hyogo-ken Nanbu earthquake in the Tamba region, central Japan. A significant increase in Q_C^{-1} following the Hyogo-ken Nanbu earthquake is detected at frequency bands from 1.5 to 4.0 Hz. A simultaneous decrease in b value is observed. The temporal variation in b value is mainly attributed to the occurrence of larger earthquakes of $M \sim 3$. This characteristic magnitude has a fault length of 400 m, in good agreement with the characteristic scale length of scatterers of 300–600 m estimated from the wavelengths of 3–4 Hz waves showing the largest significant change in Q_C^{-1}. The physical condition of the crust in the Tamba region therefore appears to be dominated by heterogeneity with a scale length of 10^2 m. The static stress change due to the Hyogo-ken Nanbu earthquake is estimated to be nearly 0.02 MPa, causing not only the change in seismicity but also the change in Q_C^{-1}. The estimated stress sensitivity of coda Q^{-1} is 10 $(\text{MPa})^{-1}$. Finally, we believe that coda Q^{-1} can be considered a reliable indicator of the stress in the crust if stable estimation is performed using a large number of stations.

Acknowledgment. We are grateful to Teruyuki Asada and Katsuyoshi Ito of the Abuyama Observatory for their assistance in collecting waveform data. Many useful comments by Anshu Jin, Rachel Abercrombie, and an anonymous reviewer are greatly appreciated. Some figures are drawn using Generic Mapping Tool (GMT) version 3 [*Wessel and Smith*, 1995].

References

Akamatsu, J., Attenuation property of coda parts of seismic waves from local earthquake, *Bull. Disaster Prev. Res. Inst. Kyoto Univ*., *30*, 1–6, 1980.

Aki, K., Maximum likelihood estimate of b in the formula $\log N = a - bM$ and its confidence limits, *Bull. Earthquake Res. Inst. Univ. Tokyo*, *43*, 237–239, 1965.

Aki, K., Scattering and attenuation of shear waves in the lithosphere, *J. Geophys. Res*., *85*, 6496–6504, 1980.

Aki, K., Theory of earthquake prediction with special reference to monitoring of the quality factor of the lithosphere by the coda method, *Earthquake Predict. Res*., *3*, 219–230, 1985.

Antolik, M., R. M. Nadeau, R. C. Aster, and T. V. McEvilly, Differential analysis of coda Q using similar microearthquakes in seismic gaps, part 2, Application to seismograms recorded by the Parkfield high resolution seismic network, *Bull. Seismol. Soc. Am*., *86*, 890–910, 1996.

Aster, R. C., G. Slad, J. Henton, and M. Antolik, Differential analysis of coda Q using similar microearthquakes in seismic gaps, part 1, Techniques and application to seismograms recorded in the Anza seismic gap, *Bull. Seismol. Soc. Am*., *86*, 868–889, 1996.

Beroza, G. C., A. T. Cole, and W. L. Ellsworth, Stability of coda wave attenuation during the Loma Prieta, California, earthquake sequence, *J. Geophys. Res*., *100*, 3977–3987, 1995.

Chouet, B., Temporal variation in the attenuation of earthquake coda near Stone Canyon, California, *Geophys. Res. Lett*., *6*, 143–146, 1979.

DeFazio, T. L., K. Aki, and J. Alba, Solid Earth tide and change in the in situ seismic velocity, *J. Geophys. Res*., *78*, 1319–1322, 1973.

Hashimoto, M., Static stress changes associated with the Kobe earthquake: Calculation of changes in Coulomb failure function and comparison with seismicity change (in Japanese with English abstract), *J. Seismol. Soc. Jpn*., *48*, 521–530, 1996.

Hashimoto, M., Correction to "Static stress changes associated with the Kobe earthquake: Calculation of changes in Coulomb failure function and comparison with seismicity change" (in Japanese with English abstract), *J. Seismol. Soc. Jpn*., *50*, 21–27, 1997.

Hashimoto, M., T. Sagiya, H. Tsuji, Y. Hatanaka, and T. Tada, Coseismic displacements of the 1995 Hyogo-ken Nanbu earthquakes, *J. Phys. Earth*, *44*, 255–279, 1996.

Hiramatsu, Y., M. Ando, and F. Takeuchi, Correlation between coda Q^{-1} and seismicity in central Japan, *Bull. Disaster Prev. Res. Inst. Kyoto Univ*., *42*, 95–114, 1992.

Horikawa, H., K. Hirahara, and Y. Umeda, Simultaneous inversion of geodetic and strong-motion data for the source process of the Hyogo-ken Nanbu, Japan, earthquake, *J. Phys. Earth*, *44*, 455–471, 1996.

Iio, Y., Scaling relation between earthquake size and duration of faulting for shallow earthquakes in seismic moment between 10^{10} and 10^{25} dyne · cm, *J. Phys. Earth*, *34*, 127–169, 1986.

Iio, Y., Depth-dependent change in the focal mechanism of shallow earthquakes: Implications for brittle-plastic transition in a seismogenic region, *J. Geophys. Res*., *101*, 11,209–11,216, 1996.

Ito, K., Regional variations of the cutoff depth of seismicity in the crust and their relation to heat flow and large inland-earthquakes, *J. Phys. Earth*, *38*, 223–250, 1990.

Jin, A., and K. Aki, Temporal change in coda Q^{-1} before the Tangshan earthquake of 1976 and the Haicheng earthquake of 1975, *J. Geophys. Res*., *91*, 665–673, 1986.

Jin, A., and K. Aki, Spatial and temporal correlation between coda Q^{-1} and seismicity and its physical mechanism, *J. Geophys. Res*., *94*, 14,041–14,059, 1989.

Katao, H., N. Maeda, Y. Hiramatsu, Y. Iio, and S. Nakao, Detailed mapping of focal mechanisms in/around the 1995 Hyogo-ken Nanbu earthquake rupture zone, *J. Phys. Earth*, *45*, 105–119, 1997.

Mori, J., and R. E. Abercrombie, Depth dependence of earthquake frequency-magnitude distributions in California: Implications for rupture initiation, *J. Geophys. Res*., *102*, 15,081–15,090, 1997.

Rautin, T. G., and V. I. Khalturin, The use of coda for determination of the earthquake source spectrum, *Bull. Seismol. Soc. Am*., *68*, 923–948, 1978.

Reasenberg, P., and K. Aki, A precise, continuous measurement of seismic velocity for monitoring in situ stress, *J. Geophys. Res*., *79*, 399–406, 1974.

Robinson, R., Temporal variation in coda duration of local earthquakes in the Wellington region, New Zealand, *Pure Appl. Geophys*., *125*, 579–596, 1987.

Sato, H., Energy propagation including scattering effects: Single isotropic scattering approximation, *J. Phys. Earth*, *25*, 27–41, 1977.
Sato, H., Temporal change in scattering and attenuation associated coda waves: A review of recent studies on coda waves, *Pure Appl. Geophys*., *126*, 465–498, 1988.
Singh, S., and R. B. Herrmann, Regionalization of crustal coda Q in the continental United States, *J. Geophys. Res*., *88*, 527–538, 1983.
Watanabe, H., Determination of earthquake magnitude at regional distance in and near Japan (in Japanese with English abstract), *J. Seismol. Soc. Jpn*., *24*, 189–200, 1971.
Wessel, P., and W. H. F. Smith, New version of the Generic Mapping Tools released, *Eos Trans. AGU*, *76*, 329, 1995.
Yomogida, K., and R. Benites, Relation between direct wave Q and coda Q: A numerical approach, *Geophys. J. Int*., *123*, 471–483, 1995.

M. Furumoto and Y. Hiramatsu, Department of Earth Sciences, Faculty of Science, Kanazawa University, Kakuma, Kanazawa 920-1192, Japan. (furumoto@hakusan.s.kanazawa-u.ac.jp; yoshizo@hakusan.s.kanazawa-u.ac.jp)
N. Hayashi, Fujitsu FIP Co., Nagoya 450-0002, Japan.
H. Katao, Research Center for Earthquake Prediction, Disaster Prevention Research Institute, Kyoto University, Gokasho, Uji 611-0011, Japan. (katao@rcep.kyoto-u.ac.jp)

(Received March 18, 1999; revised November 18, 1999; accepted November 23, 1999.)